Supplementary Data

1. Supplemental Methods
    1.1. Western blot validation of overexpression

Two female P0 C57BL/6J mouse pups were exposed to AAV using the BREVI method. One pup was exposed to AAV2-CaMKII-B4-eGFP-WPRE and the second injected with control AAV. On P21 these two mice plus one injection naïve female C57BL/6J were anesthetized, transcardially perfused and brains extracted and rapidly frozen. Bilateral cortical tissue from each brain was separated from the cerebellum and cortex anterior to A1. This tissue was combined with Tris-HCl (pH 7.4) and homogenized in lysing tubes in a bead mill. The samples were combined with 2% SDS, probe sonicated, vortexed for at room temperature at 1400RPM followed by 14,000g centrifugation. Protein concentration was estimated using a Micro BCA Protein Assay Kit (ThermoFisher Scientific #23235) (R^2 values > 0.99 for each sample). Protein levels were resolved by combining 20μg protein samples with 1x Loading Buffer (Li-Cor #928-40004) loaded into a 4-20% SDS-PAGE gradient gel (ThermoFisher Scientific #26224) and separated in 1xSDS running buffer (Pierce #28368) at 75V. Samples were transferred to a polyvinylidene fluoride membrane (Millipore #PFL00010) in 1xTris Glycine Blotting Buffer (Pierce #28363) at 4°C at 85V. Non-specific binding was reduced by incubating the membrane in Odyssey Blocking Buffer (Li-Cor #927-4000) diluted in 1x TBS. Membranes were incubated overnight in Blocking Buffer (Pierce #37353) with 0.1% Tween 20 (Sigma #P7949) and validated primary antibodies: mouse anti-Ca_Vβ4 (Neuromab #75-054, 1:1000) and rabbit anti-β-tubulin (Abcam #ab6046, 1:600,000). The membrane was incubated in Li-Cor Blocking Buffer diluted 1:1 with TBS (0.1% Tween 20 and 0.02% SDS) and IRDye secondary antibodies: goat anti-mouse 800 (Li-Cor #926-32210, 1:10,000) and goat anti-rabbit 680nm (Li-Cor #926-68071, 1:10,000). β4 isoforms were present at bands ~37.5-59kD. Signal intensity was calculated by normalizing the optical density of β4 to β-tubulin for each technical replicate. Mean optical density for β4OE, CN and AAV Naïve were calculated by averaging β-tubulin normalized technical replicates. Mean optical density of β4OE versus AAV Naïve and β4OE versus CN were evaluated via t-test.

    1.2. Sampling, Confocal Imaging and Image Processing

Images of mounted tissue sections were captured using an Olympus BX51 WI upright microscope with a spinning disk confocal, Hamamatsu ORCA R2 CCD camera, BioPrecision2 XYZ motorized stage with linear XYZ encoders (Ludl Electronic Products Ltd.), Lumen 220 light source (Prior Scientific), Ludl excitation and emission filter wheels and a Sedat Quad 89000 filter set (Chroma Technology Corp.) controlled by Slidebook6 software (Intelligent Imaging Innovations). 2-D images of each tissue section were acquired using an Olympus PlanAPO 1.25x/0.04 N.A. objective and epifluorescent 405nm and 568nm excitation. L5 mCherry+ pyramidal cells with somal GFP fluorescence, i.e. GFP+mCherry+ cells, were identified using an Olympus UPlanSApo 10x/0.40 N.A. objective and captured in 2-D at fixed exposure times (405nm=100ms, 488nm=1500ms and 568nm=150ms at 1.5% Neutral Density). These cells (n=170) were then captured in 3-D image stacks using an Olympus PlanApo N 60x/1.40 N.A. oil immersion super-corrected objective with spinning disk unit engaged. Each 60x 3-D stack comprised the cell body of one L5 pyramidal cell and all of its corresponding basal dendrites visible within the 1024x1024 pixel capture window. Neutral Density filter and exposure time for the 568nm channel were optimized for one randomly selected minor basal dendritic segment at each site for each 3-D stack captured. Minor basal dendritic segments were defined as any dendritic segment branching directly off a major or primary basal dendrite. Total tissue thickness was estimated by measuring anti-NeuN labeling in the z-dimension. 3-D image stacks were acquired through the entire thickness of the tissue (0.25μm between each z-plane).

mCherry+ fluorescent minor basal dendritic segments >50μm in length, located >10μm away from the cell body and >3μm from a dendrite branch point were identified in 1024x1024 image stacks and cropped into individual image stacks containing one minor basal dendritic segment. Mean (SD) distance

from the soma of dendritic segments captured for GFP+mCherry+ cells was 15.85 (4.48)μm, indicating dendritic segments were on proximal branches. Mean distance from soma did not significantly differ by group or sex (data not shown). Dendritic segment lengths were measured in Slidebook6 using the line tool. Individual dendritic segments were exported as TIFF series from Slidebook6 and viewed in Stereo Investigator (MBF Bioscience) software for spine counting and categorization.

1.3. Dendritic spine volume assessment

Two neurons per CN or β4OE mouse were randomly selected from among all neurons that had DSD within 2 standard deviations of the group mean for further assessment to determine if the significant main effect of group on mean DSD could be driven by a significant difference in density of spines of a particular volume. Spine objects included in the neuron DSD calculation were marked, files coded to blind investigator to neuron and group/sex, and each spine (n=1543 objects) was manually masked using the brush tool in Slidebook6 (**Supplemental Figure 2D**). Object volume (μm^3) statistics were extracted for each mask. Spine objects were organized into 10 size bins based on volume[1]. The bin with the smallest spines comprised objects of <0.1μm^3 volume, the next bin of spines volumes was from 0.1-0.2μm^3 and so on. Dendritic protrusions were classified into one of eight types: short stubby, long stubby, short mushroom, long mushroom, thin, branched or atypical dendritic spine or filopodia. Protrusion type was determined based on morphological characteristics (**Supplemental Figure 2E**)[2-4].

1.4. SDS-PAGE and Western Blot

β protein levels in male and female C57BL/6J wildtype mouse A1 were assessed at two time points relevant to the developmental period of interest for schizophrenia onset[2,5,6]: P28, which is associated with murine adolescence/estrous cycle commencement (~P24-P30) and P84, corresponding to murine adulthood. Four male and four female mice in each age group were anesthetized and brains extracted. Mouse A1 tissue was manually cut from bilateral cryostat sections and combined with SDS extraction buffer (0.125-M Tris-HCl [ph 7], 2% SDS and 10% glycerol) and centrifuged. Protein was extracted and protein concentration estimated using a Micro BCA Protein Assay Kit (ThermoFisher Scientific #23235) (R^2 values > 0.99 for each sample). Protein levels were resolved by combining 20μg protein samples with 1x Loading Buffer (Li-Cor #928-40004) loaded into a 4-20% SDS-PAGE gradient gel (ThermoFisher Scientific #26224) and separated in 1xSDS running buffer (Pierce #28368) at 75V. Samples were transferred to a polyvinylidene fluoride membrane (Millipore #PFL00010) in 1xTris Glycine Blotting Buffer (Pierce #28363) at 4°C at 85V. Membranes were incubated in Odyssey Blocking Buffer (Li-Cor #927-4000) diluted in 1xTBS. β-tubulin (50kD) was the loading control. Membranes were incubated overnight in Blocking Buffer with validated primary antibodies: either mouse anti-Ca_Vβ1 (Neuromab #73-052 1:100), rabbit anti-Ca_Vβ3 (Alomone Labs #AAC-008, 1:800) or mouse anti-Ca_Vβ4 (Neuromab #75-054, 1:1000) and rabbit anti-β-tubulin (Abcam #ab6046, 1:600,000). Then membranes were incubated in Li-Cor Blocking Buffer diluted 1:1 with TBS (0.1% Tween 20 and 0.02% SDS) and Li-Cor IRDye secondary antibodies: either goat anti-mouse 800nm (#926-32210, 1:10,000) and goat anti-rabbit 680nm (#926-68071, 1:10,000) or goat anti-rabbit 800nm (#926-32211, 1:10,000) and goat anti-mouse 680nm (#926-68070, 1:10,000).

2. Supplemental Figures

Supplemental Figure 1

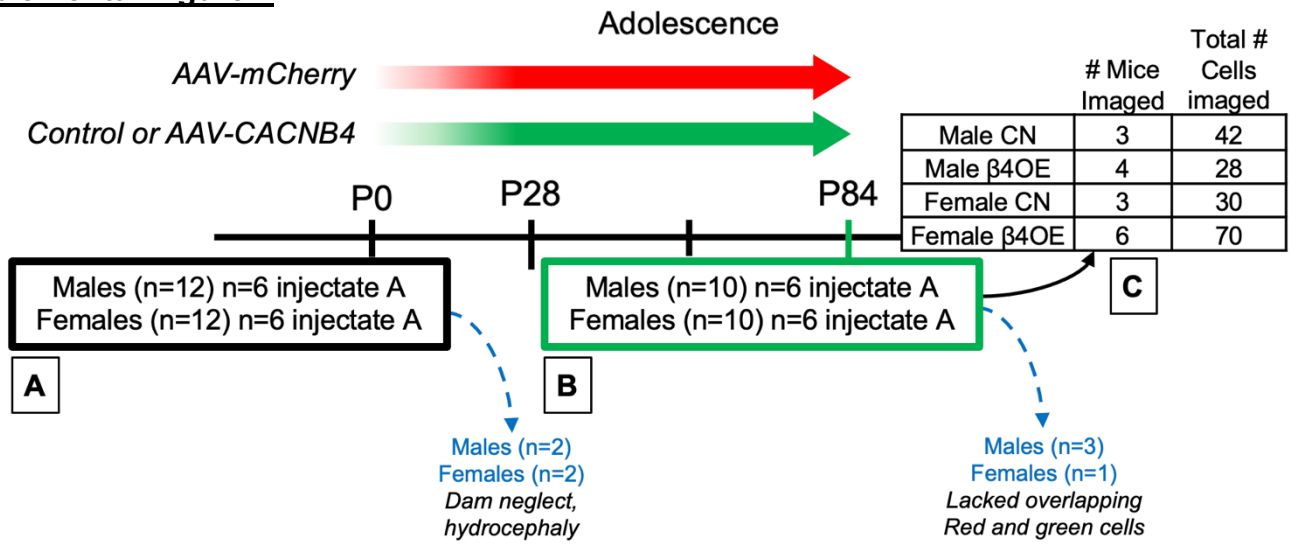

	# Mice Imaged	Total # Cells imaged
Male CN	3	42
Male β4OE	4	28
Female CN	3	30
Female β4OE	6	70

Supplemental Figure 1 Dendritic spine study design and execution. **A)** Two versions of AAV injectate were prepared by adding AAV-mCherry to either control GFP AAV (to generate control [CN] mice) or AAV-CACNB4 (to generate β4 overexpression [β4OE] mice). To blind experimenter to group AAV solutions were randomly coded "A" and "B" prior to AAV injections. Twenty-four P0-P2 C57BL/6J mouse pups were exposed to AAV injectate (50% to injectate A) using the BReVI procedure. Two males and two females perished prior to P84 due to either dam neglect (n=3) or hydrocephaly (n=1). **B)** Stage of estrous cycle was estimated by evaluating vaginal cytology of P84 females on day of sacrifice. Twenty total mice were euthanized on P84: 4 male CN, 6 male β4OE, 4 female CN, and 6 female β4OE mice. Mice were anesthetized and transcardially perfused with ice-cold 1x PBS followed by 4% PFA. Brains were extracted, post-fixed in 4% PFA, moved to 18% sucrose and stored at -30°C in cryoprotectant until sectioning. **C)** Layer 5 (L5) mCherry fluorescent pyramidal cells with GFP somal labeling (GFP+mCherry+ cells) were selected for imaging. A sparse labeling approach was utilized to specifically avoid over-sampling spines, with the tradeoff that 4 (1 male CN, 2 male β4OE and 1 female CN) of the 20 total mice euthanized were excluded from this assessment prior to image analysis, due to paucity of GFP+mCherry+ cells visible at 10x. Sixteen total mice were assessed and for each mouse all GFP+mCherry+ cells visible at 10x were imaged: 3 male CN (n=42 total cells), 4 male β4OE (n=28 cells), 3 female CN (n=30 cells) and 6 female β4OE mice (n=70 cells). We conducted DSD analyses at mouse and neuron levels, focusing on the latter, since group sizes with n=cell were better balanced, providing the ability to test sex effects.

Supplemental Figure 2

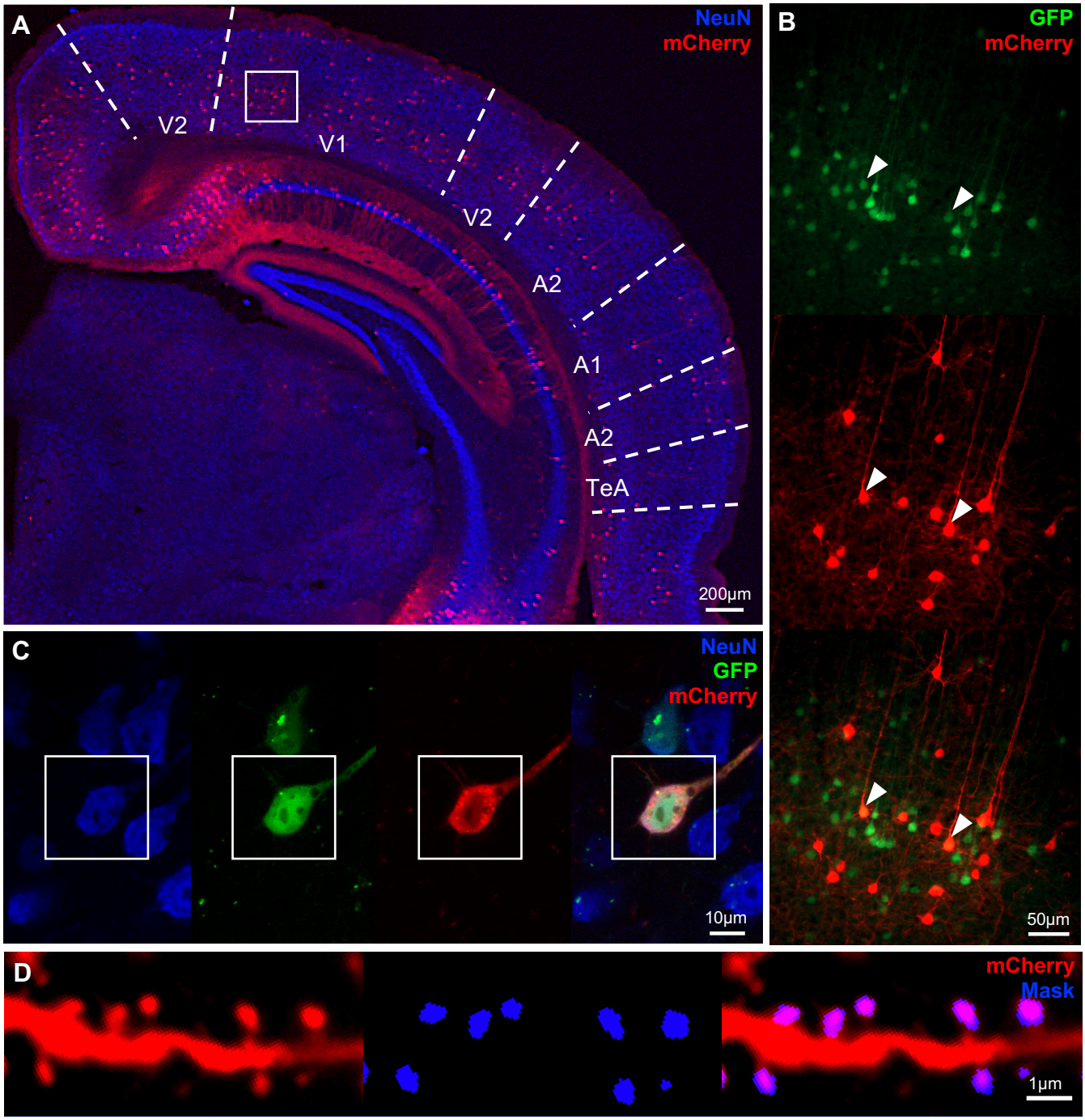

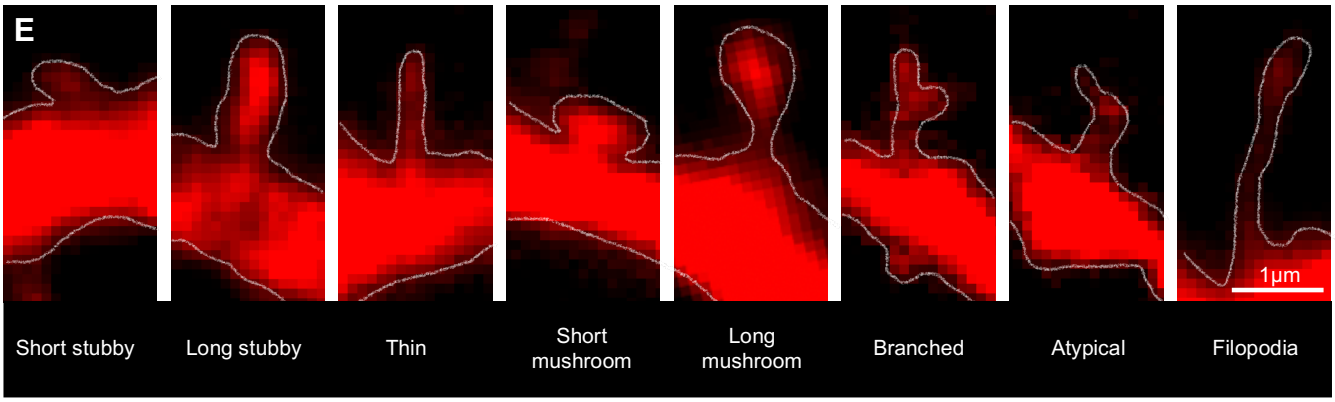

Supplemental Figure 2 Neuron sampling and image processing methods. **A)** 1.25x 2-D image of ROI including five regions of sensory cortex of a male CN mouse in the study. NeuN (blue) and mCherry but not GFP fluorescence visible at 1.25x. Dashed lines designate atlas-determined region boundaries and white box in V1 outlines 10x image of L5 pyramidal cells shown in **B**. Scalebar = 200µm. **B)** 10x 2-D image of L5 pyramidal cells with GFP (top) and mCherry (middle) fluorescence. White carets point out the two L5 pyramidal cells with the highest GFP+mCherry+ (merge, bottom) fluorescent intensity. Scalebar = 50µm. **C)** 60x 2-D image of GFP+mCherry+ pyramidal cell from Ms8-164. White box outlines the cell body of the L5 pyramidal cell of interest. Merge far right. Scalebar = 10µm. **D)** Masking strategy used to calculate dendritic spine object volume. For two neurons per mouse, each spine included in neuron DSD was manually marked in Slidebook6. Then, each marked spine object was manually masked using the brush tool in Slidebook6 in the 3D planes in which it occurred. Far left panel shows a 2-D image (single z-plane) of an unmasked representative dendritic segment with dendritic protrusions from Neuron 3 of Ms6-114. Middle panel shows the mask only for the protrusions on this dendritic segment. Far right panel shows the merge. Scalebar = 1µm. **E)** Dendrite protrusion category examples. Scalebar = 1µm.

Supplemental Figure 3

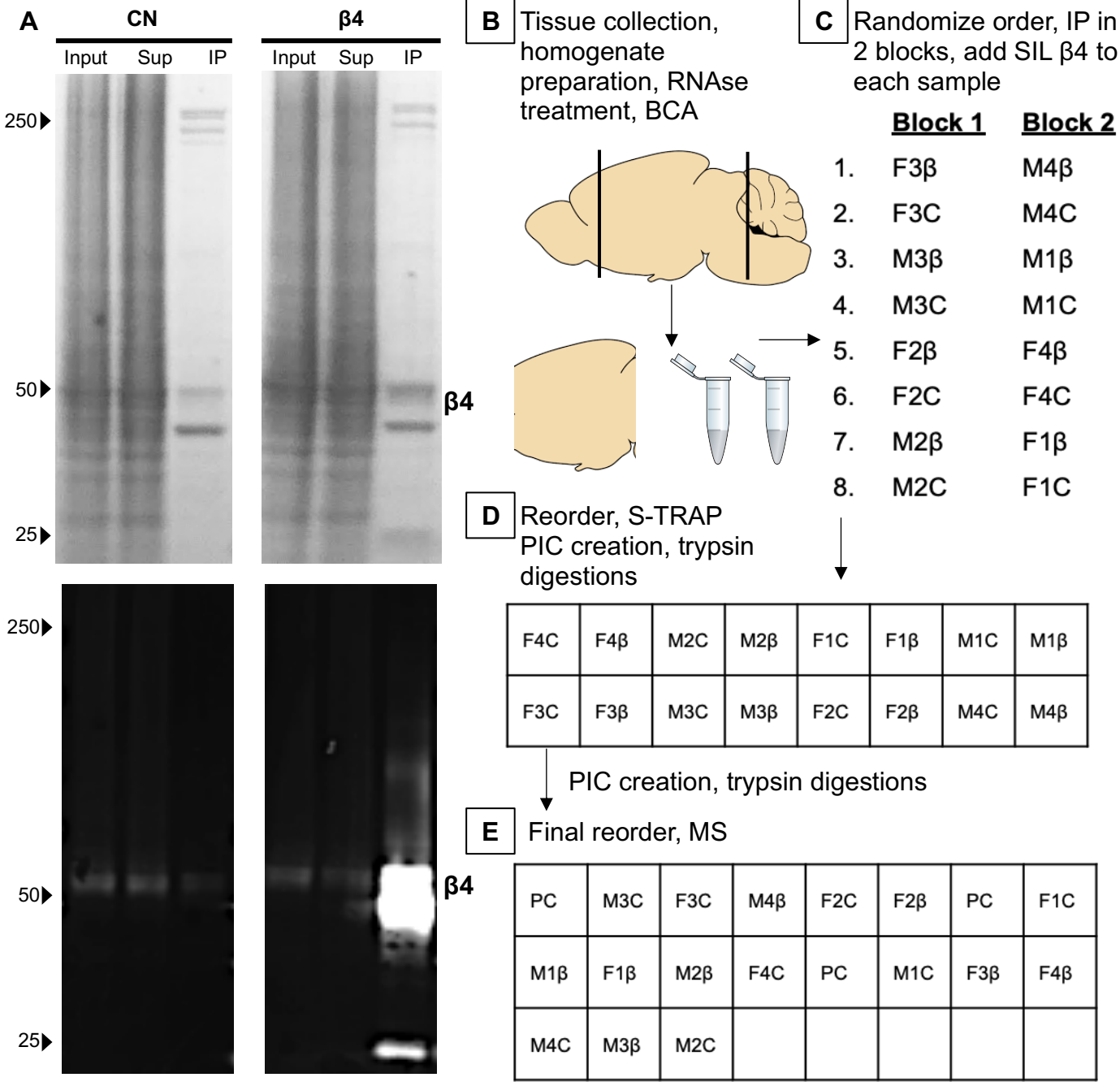

Supplemental Figure 3 Co-IP and CoIP-MS methods. **A)** (Above) β4 was immunoprecipitated from RNAse treated mouse brain lysate (n=1 adult female C57Bl/6J mouse) using 10μg mouse anti-Ca_Vβ4 antibody (Neuromab #75-054) per 1mg beads (Input=lysate prior to antibody coupling, Sup=supernatant, IP=immunoprecipitant) run out on a gel. Non-antibody coupled beads were used as negative control (CN). β4 isoforms are present at 37.5-59kD (predominant isoforms at ~55kD). (Below) β4 and β4-IP proteins using anti-Ca_Vβ4 antibody (Neuromab #75-054) and detection with a goat anti-CACNB4 antibody (Everest Biotech #EB06591, 1:1000) and donkey anti-goat 800 secondary antibody (LiCor #926-32214, 1:10,000). CoIP-MS study design in **B-E**. **B)** For each brain, bilateral cerebral cortex and underlying structures were separated from the olfactory bulb at the optic chiasm, and tissue posterior to the cerebral cortex, midbrain junction. Mouse brain tissue was homogenized using Triton x-100 lysis buffer, treated with RNAse and total protein amount determined using BCA. **C)** Sample name abbreviations were created e.g. Female mouse #3 β4-IP (F3β), Male #1 CN (M3C), and immunoprecipitation (IP) run in two blocks with sample pairs in random order. 1μL stable isotope

labeled (SIL) β4 protein was added to each sample (samples=16). Note: sample tubes were number coded starting during this step to blind experimenter to group. Sample name abbreviations rather than number codes are used in schematic to increase clarity. **D)** Samples were reordered, and S-TRAP performed. A pooled instrument control (PIC) was created from all samples and each sample digested with trypsin. **E)** Samples were reordered a final time and loaded onto the LC-MS for analysis.

Supplemental Figure 4

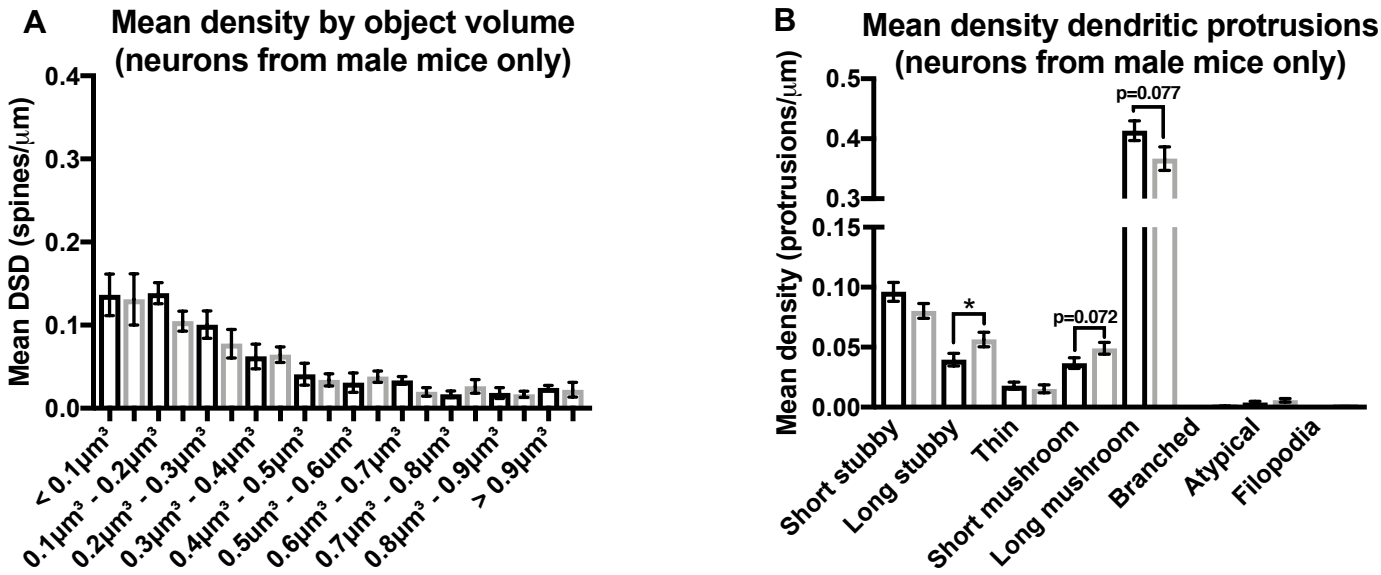

Supplemental Figure 4 Impact of β4OE on dendritic spines of male mice. **A)** Unlike in females, in male mice β4OE did not significantly reduce mean DSD of masked objects with small < 0.1μm^3 volume ($F=0.017$, $DF=1$, $p=0.900$). Genotype also did not significantly alter mean DSD of masked objects of 0.1μm^3 - 0.2μm^3 volume in male mice ($F=3.620$, $DF=1$, $p=0.81$). Error bars = SEM. **B)** β4OE significantly increased mean density of long stubby spines in male mice ($F=4.202$, $DF=1$, $p=0.044$). There was a trend level increase in mean density of short mushroom ($F=3.332$, $DF=1$, $p=0.072$) and a trend level decrease in mean density of long mushroom ($F=3.215$, $DF=1$, $p=0.077$) spines in male β4OE mice. Error bars = SEM.

3. Supplemental Tables

Supplemental Table 1

Peptide	Protein ID	β4-IP Mean	Negative CN Mean	Log2(β4-IP)-Log2(CN)	p value
ILLDAGFTNELVQNYWSK	CA2D1	4679428.52	430883.648	3.44096209	0.0020032
HLNVQIAASEK	CACB1	1972810.91	575075.819	1.7784286	0.000678
EGGDIAFIPSPQR	CACB3	12280054.2	1034063.14	3.56992075	0.00132655
TSLAPIIVHVK	CACB4	220800749	4296093.28	5.68357594	6.6278E-06
GSSAGFLTLHNAFPK	CCG8	26893944.7	2476365.74	3.44098507	2.2347E-05
GPDGEPQPGLESQGR	CAC1B	3660770.58	984309.532	1.89496339	0.07737068
SKTDLLNPEEAEDQLADIASVGSPFAR	CAC1A	7684689.21	1429661.12	2.42631369	0.00037217
SLFIFGEDNIVR	CAC1E	15626148.1	1367039.48	3.51483538	4.2502E-05
HASLDGASPYFK	CBARP	7077283.81	386774.592	4.19363085	0.00011575
LADFGLAIEVEGEQQAWFGFAGTPGYLSPEVLR	KCC2A	16655492.9	4292426.25	1.9561328	0.00029843
NSLVSPAQEPAPLQTAMEPQTTVVHNATDGIK	KCC2G	11039219.1	3554233.61	1.6350277	0.00211111
WQNVHFHCSGAPVAPLQ	KCC2B	48924331.4	8320871.35	2.55574562	0.00031296
VTEQLIEAINNGDFEAYTK	KCC2D	170897637	51071238.1	1.74254951	9.0052E-05
HIFALFNTEQR	DYN1	1337059441	248763365	2.42621766	5.726E-05
NLVDSYVAIINK	DYN2	26011838.4	4424921.46	2.55544462	0.00036523
DFINSELLAQLYSSEDQNTLMEESAEQAQR	DYN3	4692986.01	844595.315	2.47417401	3.1317E-06
GPGPLQER	MATR3	9081529.79	1012921.79	3.16441255	0.00030925
ELIFEETAR	MK01	19980737	5684580.29	1.81348406	0.00049902
YAGLTFPK	MK10	47936716.2	11171215.2	2.10134495	0.0006719
EIQILLR	MK03	26591656.5	5242495.99	2.34264789	0.00012184
NIIGLLNVFTPQK	MK08	18472179	3011726.26	2.61669151	6.4344E-05
KLIHLEIKPAIR	MP2K1	7366876.12	699448.954	3.3967623	0.00061777
LQGTHYSVQSDIWSMGLSLVELAIGR	MP2K2	9130170.09	595500.023	3.93846827	4.9442E-05
SDVWSLGITLYELATGR	MP2K4	14163070.2	1889143.79	2.90632961	5.4254E-05
ILANGQMNEQDIR	MP2K5	1688528.28	158518.721	3.4130412	0.02430607
EAFEQPQTSSTPPR	MP2K6	12080013.4	1895764.2	2.67177063	0.00155127
DVKPSNILLDER	MP2K7	21391015.4	4721868.32	2.17957525	0.0001709
SLLAAQQTFVDR	PK3C3	14133065.9	2561537.4	2.4639926	0.0003328
TLVTGGATPELEALIAEENALR	KCMA1	15441800	4596895.79	1.74810907	0.00029363
KGTEELYAIK	KPCA	17227148.3	3350753.57	2.36212641	3.603E-05
DIKEHAFFR	KPCB	125821888	30482936.7	2.04530912	0.00024614
SEEEAKFPTMNR	KPCD	3634260.09	746119.948	2.28418219	0.00059478
LAAGAESPQPASGNSPSEDDRSK	KPCE	25555749.4	3750681.52	2.76842323	8.7931E-06
LVLASIDQADFQGFTYVNPDFVHPDAR	KPCG	119358003	34747156.5	1.78032847	8.6122E-05
DVVLMDDDVECTMVEK	KPCT	33955244.7	3786334.84	3.16476053	0.02319497
YFAQEALTVLSLA	2AAA	60900968.3	17238564.7	1.82082551	7.5425E-05
FFEEPEDPSSR	2ABD	13957147.7	3499596.63	1.99574359	0.00284384
INLWHLAITDR	2ABG	7969074.15	1967713.85	2.01789169	7.9454E-05

EAPVPRPTPQVAASGGQS	2A5B	5852125.35	1087748.13	2.42761614	0.00019822
ELFEGAVR	REM2	30209737.4	13006994.4	1.21572601	0.00392079
YVDEAHQYILEFDGGSR	RYR2	11191113.9	2322597.47	2.26854259	7.9859E-05
EINDLAESGAR	RYR3	161878090	1147912.95	7.13975068	8.677E-05
ESALILLQTVPK	ZNT1	4402207.23	1475242.63	1.5772748	0.01102076
SLFTEPSEPLPEEPK	ZNT3	33314252.1	4630270.12	2.84697124	8.3469E-05
LTELLESDPSVR	ZNT9	4013997.57	744806.691	2.43010181	0.06512629
LLTNLGLGEIK	S39AA	8379085.3	1143707.33	2.87307485	0.00157128
NTLNPYYNESFSFEVPFEQIQK	SYT1	126552581	15797161.5	3.00199967	8.6181E-05
VPMNTVDLGQPIEEWR	SYT2	16821234.5	2471263.78	2.76696267	0.00022299
YDYESETLIVR	SYT6	12489316.5	2271135.4	2.4592089	4.5682E-05
IYLLPDKK	SYT7	5776414.96	764432.873	2.91771266	2.751E-05
GELQVSLSYQPVAQR	SYT11	5802165.07	1491297.49	1.96002326	0.003395
VSLLPDEQIVGISR	SYT12	45324978.2	7494428.56	2.59641594	2.6405E-05
TGSVEAQTALK	SYT13	17223089.9	3194783.8	2.43055378	0.00041057
QLLQTDVSQGSDPFVK	SYT17	7371700.44	2053695.22	1.84377535	0.00040559

Supplemental Table 1

Table with VGCCs and other previously reported β-interacting proteins identified within the β4 interactome of male and female P84 mice. In nearly all cases, multiple peptides per Protein ID were identified. Peptide with the lowest significant p value per Protein ID is reported. As expected, the VGCC subunits $Ca_V2.1$, $Ca_V2.2$, $Ca_V2.3$ and $\alpha_2\delta1$ were identified in the list of protein/peptides detected using the CoIP LC-MS approach utlized in the current study. Furthermore, ryanodine receptors 1 and 2 were identified in the present as well as previously published studies as were dynamin 1-3, phosphoinositide 3-kinase (PI3K), calcium/calmodulin-dependent kinase II (CaMKII, protein ID label KCC2), members of the synaptic protein family synaptotagmin, zinc transporter 1 (plus zinc transporter 3, 9 and 10), members of the Mitogen-activated protein kinase (MAPK) and MAPK kinase families (protein ID labels MK and MP2K), members of the Protein Kinase C family of proteins and the relatively recently discovered and described β-anchoring and-regulatory protein (BARP)[7-19].

4. Supplemental References

1 MacDonald, M. L. *et al.* Selective loss of smaller spines in schizophrenia. *American Journal of Psychiatry* **174**, 586-594 (2017).

2 Parker, E. M., Kindja, N. L., Cheetham, C. E. J. & Sweet, R. A. Sex differences in dendritic spine density and morphology in auditory and visual cortices in adolescence and adulthood. *Scientific Reports* **10**, 1-11, doi:10.1038/s41598-020-65942-w (2020).

3 Arellano, J. I., Benavides-Piccione, R., DeFelipe, J. & Yuste, R. Ultrastructure of dendritic spines: correlation between synaptic and spine morphologies. *Frontiers in Neuroscience* **1**, 131-143 (2007).

4 Risher, W. C., Ustunkaya, T., Alvarado, J. S. & Eroglu, C. Rapid Golgi analysis method for efficient and unbiased classification of dendritic spines. *PLoS One* **9**, e107591, doi:10.1371/journal.pone.0107591 (2014).

5 Caligioni, C. S. Assessing reproductive status/stages in mice. *Current Protocols in Neuroscience, Appendix 4* **48**, Appendix-4I (2009).

6 Moyer, C. E. *et al.* Developmental trajectories of auditory cortex synaptic structures and gap-prepulse inhibition of acoustic startle between early adolescence and young adulthood in mice. *Cerebral Cortex* **26**, 2115-2126 (2015).

7 Cheng, W., Altafaj, X., Ronjat, M. & Coronado, R. Interaction between the dihydropyridine receptor Ca2+ channel β-subunit and ryanodine receptor type 1 strengthens excitation-contraction coupling. *Proceedings of the National Academy of Sciences* **102**, 19225-19230 (2005).

8 Buraei, Z. & Yang, J. The β subunit of voltage-gated Ca 2+ channels. *Physiological Reviews* **90**, 1461-1506 (2010).

9 Gonzalez-Gutierrez, G., Miranda-Laferte, E., Neely, A. & Hidalgo, P. The Src homology 3 domain of the β-subunit of voltage-gated calcium channels promotes endocytosis via dynamin interaction. *Journal of Biological Chemistry* **282**, 2156-2162 (2007).

10 Sheng, Z.-H., Westenbroek, R. E. & Catterall, W. A. Physical link and functional coupling of presynaptic calcium channels and the synaptic vesicle docking/fusion machinery. *Journal of Bioenergetics and Biomembranes* **30**, 335-345 (1998).

11 Levy, S. *et al.* Molecular basis for zinc transporter 1 action as an endogenous inhibitor of L-type calcium channels. *Journal of Biological Chemistry* **284**, 32434-32443 (2009).

12 Beharier, O. *et al.* Crosstalk between L-type calcium channels and ZnT-1, a new player in rate-dependent cardiac electrical remodeling. *Cell Calcium* **42**, 71-82 (2007).

13 Ohana, E. *et al.* Silencing of ZnT-1 expression enhances heavy metal influx and toxicity. *Journal of Molecular Medicine* **84**, 753-763 (2006).

14 Segal, D. *et al.* A role for ZnT-1 in regulating cellular cation influx. *Biochemical and Biophysical Research Communications* **323**, 1145-1150 (2004).

15 Fitzgerald, E. M. The presence of ca2+ channel β subunit is required for mitogen-activated protein kinase (mapk)-dependent modulation of α1b ca2+ channels in cos-7 cells. *The Journal of Physiology* **543**, 425-437 (2002).

16 Béguin, P. *et al.* BARP suppresses voltage-gated calcium channel activity and Ca2+-evoked exocytosis. *Journal of Cell Biology* **205**, 233-249 (2014).

17 Nakao, A. *et al.* Comprehensive behavioral analysis of voltage-gated calcium channel beta-anchoring and-regulatory protein knockout mice. *Frontiers in Behavioral Neuroscience* **9**, 141, doi:10.3389/fnbeh.2015.00141 (2015).

18 Abiria, S. A. & Colbran, R. J. CaMKII associates with CaV1. 2 L-type calcium channels via selected β subunits to enhance regulatory phosphorylation. *Journal of Neurochemistry* **112**, 150-161 (2010).

19 Grueter, C. E., Abiria, S. A., Wu, Y., Anderson, M. E. & Colbran, R. J. Differential regulated interactions of calcium/calmodulin-dependent protein kinase II with isoforms of voltage-gated calcium channel β subunits. *Biochemistry* **47**, 1760-1767 (2008).